Research Article

N. Zaheer Ahmed, G. Dicky John Davis, Asim Ali Khan, Lavanya Prabhakar, Meena Ram Paratap, Zeba Afnaan, Meera Devi Sri and Noman Anwar*

Arq Ajīb – a wonder Unani formulation for inhibiting SARS-CoV-2 spike glycoprotein and main protease – an *in silico* approach

https://doi.org/10.1515/jcim-2021-0241
Received June 5, 2021; accepted October 6, 2021;
published online October 22, 2021

Abstract

Objectives: The current pandemic caused by Severe Acute Respiratory Syndrome Corona-Virus 2 (SARS-CoV-2) has become a global health menace with significant morbidity and mortality besides huge socioeconomic implications. Despite the approval of few vaccines for the prevention of the disease, the discovery of safe and effective countermeasures especially from natural sources is of paramount importance, as the number of cases continues escalating. Arq Ajīb has long been used for various diseases and its ingredients have been reported for antiviral, antimicrobial, antipyretic, anti-inflammatory, antioxidant activities. The present study investigates the inhibitory effect of phytocompound of Arq Ajīb on potential drug targets of SARS-CoV-2.

Methods: The structures of phytocompounds present in Arq Ajīb were retrieved from PubChem database and some were illustrated using Marvin Sketch. SARS-CoV-2 S glycoprotein (PDB ID: 6LZG) and $3CL^{pro}$ (PDB ID: 7BQY) were selected as the target protein. Dock Prep module in UCSF Chimera software was used for receptor structure processing. AutoDock Vina was used to calculate the binding affinities between the protein and ligands and to predict most promising compounds with best scores.

Results: Molecular docking results predicted that the phytocompounds of Arq Ajīb had good binding affinity and interaction with S glycoprotein and $3CL^{pro}$. Quercetin and Isorhoifolin from *Mentha arvensis* were identified as promising candidates with the potential to interact with $3CL^{pro}$ and spike glycoprotein and inhibit the viral replication and its entry into the host.

Conclusions: Arq Ajīb may prove valuable for developing novel therapeutic candidate for COVID-19; however, it has to be substantiated further with *in-vitro* and *in-vivo* studies.

Keywords: Arq Ajīb; isorhoifolin; molecular docking; quercetin; SARS-CoV-2.

Introduction

The current pandemic COVID-19 caused by Severe Acute Respiratory Syndrome Corona-Virus 2 (SARS-CoV-2) has become a matter of global health concern and still continues escalating since cases were first reported in China in December 2019 [1]. As per the current statistics, more than 233 million confirmed cases of COVID-19 have been reported globally, including more than 4 million deaths [2]. India experienced a devastating second wave with rampant growth in the number of cases and reported highest number of daily cases globally during April–June 2021. As per the latest reports, more than 33 million cases have been reported in India including 448,339 deaths [3, 4]. SARS-CoV-2 belongs to the extraordinarily large single-stranded RNA coronavirus family 'Coronaviridae' with typical morphological characteristics [5]. It could infect human with symptoms highly resembles viral pneumonia like other viruses of the family such as SARS-CoV and MERS-Co-v and shares similar mode of transmission [6]. SARS-CoV-2 binds to Angiotensin-converting enzyme 2 (ACE2) receptor via receptor-binding domain (RBD) of its' spike proteins and delivers virus particle inside the host [7, 8].

***Corresponding author: Dr. Noman Anwar,** Research Officer (Unani), Regional Research Institute of Unani Medicine, N1, West Mada Church Road, Royapuram, Chennai 600013, Tamil Nadu, India,
E-mail: nanomananwar@gmail.com.
https://orcid.org/0000-0003-0327-0033
N. Zaheer Ahmed and Meera Devi Sri, Regional Research Institute of Unani Medicine, Chennai, India
G. Dicky John Davis, Lavanya Prabhakar and Zeba Afnaan, Sri Ramachandra Institute of Higher Education and Research (Deemed to be University), Chennai, India
Asim Ali Khan and Meena Ram Paratap, Central Council for Research in Unani Medicine, M/o AYUSH, Govt of India, New Delhi, India

Discovery of effective drugs is highly paramount to curb the devastating situation caused by SARS-CoV-2 as the effective targeted therapy options still remains limited for this deadly disease. Medicinal plants and their active metabolites have gained renewed attention for the development of effective medications for various diseases. Ayurveda, Unani, Siddha and other traditional systems have enormous citations on infectious diseases and epidemics, and offer a wide range of countermeasures for the control of current pandemic. A number of drugs being used for millennia in these systems of medicine are proved to have potent antiviral activities against a number of viruses [9]. Recently, a Siddha formulation was computationally evaluated for its effect against SARS-CoV-2 and exhibited a high binding affinity with SARS-CoV-2 spike protein [10]. Reports available on antiviral effect of various medicinal plants support the hypothesis that traditional drugs may also prove to be a potent therapeutic candidate against SARS-CoV-2.

Arq Ajīb, which literally means "Wonder liniment", is a compound Unani formulation containing *Satt-e-Pudina* (plant extract of *Mentha arvensis*), *Satt-e-Ajwain* (seed extract of *Trachyspermum ammi*) and Kafoor (Camphor). The formulation is claimed to be highly effective as an antispasmodic, analgesic, digestive, anti-flatulent and anti-catarrh drug candidate. Oral intake of the formulation, in a dose of 2–5 drops with water, is effective in relieving *Waja'al-Mi'da* (Gastralgia), *Waja'al Am'a'* (intestinal colic), *Qay'* (Vomiting), *Ishāl* (Diarrhea), *Hayḍa* (Food poisoning) and *Ṭā'ūn* (Plague). Its topical application on forehead helps relieve *Ṣudā'* (Headache) and Shaqīqa (migraine). Steam inhalation of Arq Ajīb (1–2 drop) alleviates *Nazla* (catarrh), *Zukam* (coryza) and nasal congestion. It is useful as an antidote in snake bite, scorpion and other poisonous insects' sting [11–14]. Despite extensive use, the formulation has hardly been investigated scientifically to substantiate the therapeutic claims. A study has reported significant antidiarrheal activity of the formulation in charcoal-induced gut transit, serotonin-induced diarrhea and PGE2-induced small intestine enteropooling in rats [15].

The ingredients of the formulation possess diverse medicinal properties. Pudina (*M. arvensis* Linn) belongs to the family Lamiaceae is a common edible and aromatic herb with wide use in pharmaceutical, cosmetic and flavoring industries [16, 17]. It has a long history of medicinal use in Unani medicine to treat diarrhea, dysentery, indigestion, liver and spleen diseases, coryza, asthma, headache, jaundice and rheumatic pain [18, 19]. Pudina has been reported to exhibit antiviral, cytotoxic [20], antimicrobial, antioxidant, analgesic, anti-inflammatory, anti-allergic, anticancer and radioprotective activities [16, 17]. Ajwain (*T. ammi* Linn – Apiaceae) is a well-recognized spice and highly valued medicinal herb. It is known to possess analgesic, antispasmodic, anti-inflammatory, antiseptic, anthelmintic, antidote, diuretic and carminative properties, and has been used in Unani medicine for fever, cough, asthma, colicky pain, dyspepsia, liver cirrhosis, chronic splenitis, hypertension, dysurea, renal stone, amenorrhea and intestinal worms in different forms [18, 19]. It has been reported for antiviral [21, 22], antimicrobial, insecticidal, antioxidant, anti-inflammatory, anti-spasmodic, bronchodilating and antitussive activities [23]. *Kafoor* (camphor) is a well-known Unani drug with considerable therapeutic value. It is a waxy, white crystalline substance derived from the wood of camphor laurel (*Cinnamomum camphora* L.) through steam distillation [24, 25]. It acts as an analgesic, antispasmodic, antipyretic, expectorant, antiseptic, anesthetic, resolvent and anti-inflammatory. In Unani medicine, it is used externally in pleurisy, pneumonia, epistaxis, otalgia, headache, toothache, lowback pain, polyarthritis and skin disorders. Internally it is used for fever, cold and cough, bronchial asthma, tuberculosis, food poisoning, diarrhea, insomnia, palpitation and dysuria [18, 19]. Camphor has been reported for antiviral, antimicrobial, insecticidal antitussive, antimutagenic, anticancer [25], anti-inflammatory, antioxidant [26] and anti-allergic activities [27].

Computational methods are efficient tools commonly employed for drug repurposing and discovery, as it shorten the lengthy process of drug discovery and development. These tools have extensively been utilized for investigating the potential biological activity of both conventional and traditional drug molecules against SARS-CoV-2 [8]. To our knowledge, the effect of Arq Ajīb against SARS-CoV-2 has not yet been explored. The present study investigates the inhibitory effect of phytoconstituents present in Arq Ajīb on potential drug targets of SARS-CoV-2, in order to identify multitarget drug candidate and to further develop potent drug for COVID-19.

Material and methods

Receptor preparation

SARS-CoV-2 S glycoprotein (PDB ID: 6LZG) and $3CL^{pro}$ (PDB ID: 7BQY) were selected as the target protein. Dock Prep module in UCSF (University of California, San Francisco) Chimera software (v1.14) was used for receptor structure processing [28]. AM1-BCC charges were computed for the receptor which is included in Chimera. The covalent bond between the Cys145 residue and the crystallized ligand in 7BQY was eliminated. Chimera software was used for protonation and optimization of His and Cys residues.

Ligand preparation

The structures of phytocompounds were retrieved from PubChem database [29] and few were illustrated using Marvin Sketch of the Marvin (v20.8.0) suite [30]. The 3D structure of the ligands was protonated and assigned AM1-BCC charges using Chimera's Dock Prep module.

Receptor-ligand docking

Molecular docking was performed using AutoDock Vina (v1.1.2) software to predict binding affinities (kcal/mol) and find the most favorable binding interactions [31]. UCSF Chimera Dock prep tool was used to prepare protein and compounds for docking. AutoDock Vina with parameter "exhaustiveness = 8" was used to calculate the binding affinities between the protein and ligands. Binding interactions were elucidated using UCSF Chimera. The search space for SARS-CoV-2 S glycoprotein was made as wide as the size of the RBD external subdomain (S438-Y505) in a grid box of (x = −37, y = 30.5, z = 6), so that the ligand could be docked to all parts of the receptor. In $3CL^{pro}$ the co-crystallized ligand N3 (PDB ID: 7BQY) within the catalytic site was taken as a reference and the search space was set with a grid box of (x = −9.5, y = 12, z = 68.5). The results were finally analyzed using BIOVIA Discovery Studio Visualizer 2020 (v20.1.0) [32].

Molecular dynamics (MD) simulation

Molecular dynamics study was performed for four ligand – protein docked complexes i.e. Quercetin-Spike glycoprotein (QCS), Isorhoifolin-Spike glycoprotein (ISS), Quercetin-Protein $3CL^{pro}$ (QCP) and Isorhoifolin-Protein $3CL^{pro}$ (ISP) using GROMACS 5.1.4 software [33]. The topology of the ligand was generated using PRODRG server [34] and Gromos96 53a6 force field [35] was applied to build protein topology. All MD simulation systems were solvated with extended simple point charge (SPC-E) water cubic box model. A total of 19,215, 19,209, 29,375 and 29,370 number of solvent molecules were added to QCS, ISS, QCP and ISP respectively. The overall charge of the system was neutralized by adding Na^+/Cl^- ions and further energy minimization was carried out using 50,000 steepest descent steps for docked complexes. Each system was equilibrated with number of particles, volume and temperature (NVT) and number of particles, pressure and temperature (NPT) for 100 ps time scale. Finally, MD simulation step was carried out to analyze the stability of docked complexes for 100 ns time scale.

The MD simulation trajectories were analyzed using GROMACS distribution tool [36] to obtain Root mean square deviation), RMSF (Root mean square fluctuation (RMSD), number of hydrogen bonds formed between protein and ligand complexes, radius of gyration (*Rg*) and Solvent Accessible Surface Area (SASA). The graphs were generated using XMgrace tool [37]. The binding free energy (ΔG_{bind}) of individual protein – ligand complex was calculated by molecular mechanics/Poisson–Boltzmann surface area (MM-PBSA) using g_mmpbsa tool [38]. The last 20 ns stable trajectories from RMSD plot of each docked complexes were selected to compute binding free energy.

Results

The phytocompounds of Arq Ajīb, retrieved from PubChem database or illustrated using Marvin Sketch include Thymol, Carvacrol, Cymene and Terpinene from *T. ammi*; Menthol, Quercetin and Isorhoifolin from *M. arvensis*; Camphor, Linalool and Borneol from *C. camphora* (Table 1).

Binding affinity and interactions of phytocompounds with S glycoprotein

The results of the molecular docking predicted docking energies of tested phytocompounds ranging from −7.9 to −4.2 kcal/mol. Nelfinavir was used as positive control with binding energy of −7.2, showing H-bonding with Glu406, Tyr453, Gly496 and Pi-Alkyl hydrophobic interactions with Leu455 and Tyr505 (Table 2). Binding affinities of phytocompounds towards active site of SARS-CoV-2 S glycoprotein was studied in detail and reported in Table 2 and 2D interaction in Table S-1 (Supplemental Material). Visualization performed for promising candidates having best binding affinity and interactions with target protein represented in Figure 1. Biological interaction of phytocompounds was analyzed in reference to key contact residues with hACE2 subdomain I and II. All the tested phytocompounds showed effective binding interactions with S glycoprotein. Two phytocompounds 'Quercetin and Isorhoifolin' from *M. arvensis* exhibited binding energy of −6.7 and −7.9 respectively. Isorhoifolin showed interactions with amino acid residues Arg403, Glu406, Lys417, and Tyr505 that played significant role in H-bond network formation.

Binding affinity and interactions of phytocompounds with $3CL^{pro}$

The $3CL^{pro}$ is a cysteine protease which presents a unique Cys-His catalytic dyad (His41 and Cys145) at its active site. The amino acid residues 'Thr190, Glu166, Phe140, Gln189 and His164' seem to play important role in the interaction [39], hence, these residues were targeted to assess the molecular docking score and binding interactions. The results of the molecular docking predicted docking energies of tested phytocompounds ranging from −8.8 to −4.1 kcal/mol. The positive control, nelfinavir showed a binding energy of −7.7 and H-bonding with His41, Glu166, Gln189 and hydrophobic interactions of Pi–Pi, Pi–Alkyl

Table 1: Chemical structures of Phytocompounds from Arq Ajīb.

No.	Name of Drugs	Phytocompounds	Chemical structures
1	Ajwain *(T. ammi)*	Thymol	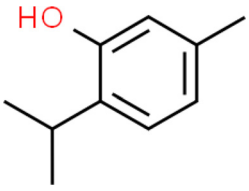
2	Ajwain *(T. ammi)*	Carvacrol	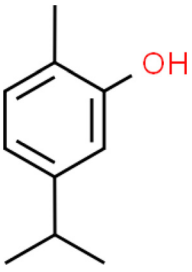
3	Ajwain *(T. ammi)*	Cymene	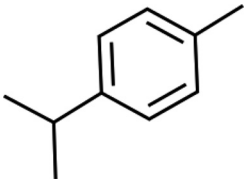
4	Ajwain *(T. ammi)*	Terpinene	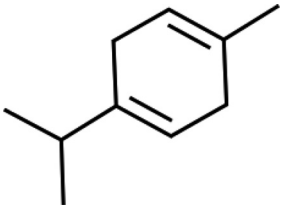
5	Pudina *(M. arvensis)*	Menthol	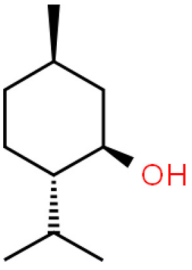
6	Pudina *(M. arvensis)*	Quercetin	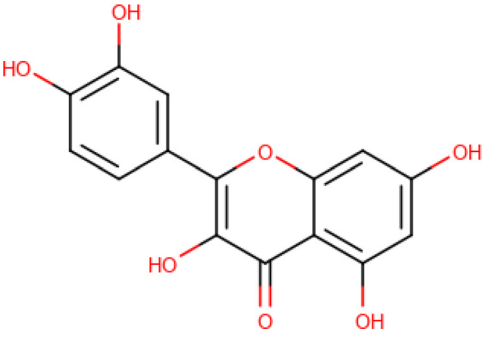

Table 1: (continued)

No.	Name of Drugs	Phytocompounds	Chemical structures
7	Pudina *(M. arvensis)*	Isorhoifolin	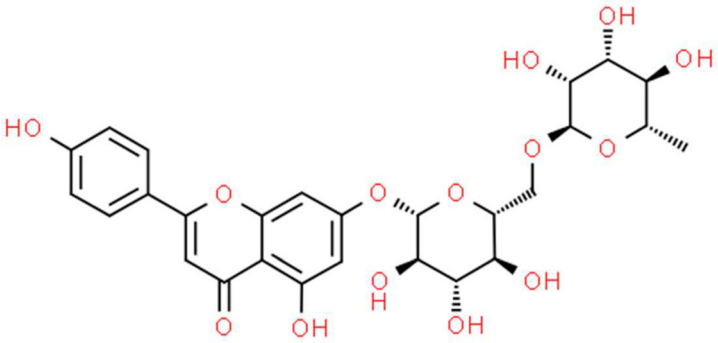
8	Kafoor *(C. camphora)*	Camphor	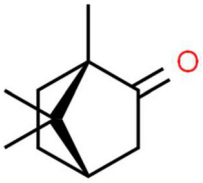
9	Kafoor *(C. camphora)*	Linalool	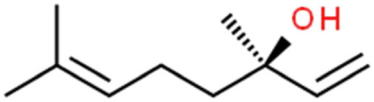
10	Kafoor *(C. camphora)*	Borneol	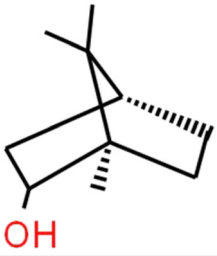

Table 2: Amino acid residues of SARS-CoV-2 S glycoprotein (6LZG) participated in H-Bond and hydrophobic interactions with ligands.

Compound	Binding energy, kcal/mol	Interactions	
		H-bonding	Hydrophobic
Nelfinavir	−7.2	Glu406, Tyr453, Gly496	Leu455, Tyr505
Thymol	−5.4	Asn501, Tyr505	Tyr453, Tyr495
Carvacrol	−5.4	Gly496, Asn501	Gly496, Tyr505
Cymene	−4.7	NHB	Gly496
Terpinene	−4.7	NHB	Tyr453, Tyr495, Tyr505
Menthol	−5.2	Gly496, Asn501	Tyr453, Tyr495, Tyr505
Quercetin	−6.7	Arg403, Gln493, Gly496, Asn501	Tyr453, Tyr505
Isorhoifolin	−7.9	Arg403, Glu406, Lys417, Tyr505	Arg403, Tyr453, Tyr505
Camphor	−4.2	NHB	Tyr495
Linalool	−4.7	NHB	Arg403, Tyr495, Phe497, Tyr505
Borneol	−4.7	NHB	Arg457, Pro491

NHB, no hydrogen bond interactions.

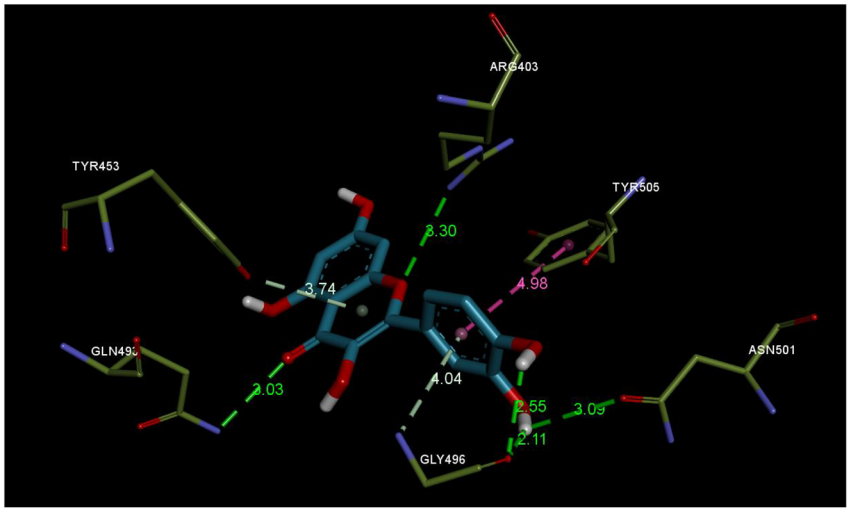

QuercetinΔG -6.7 kcal/mol

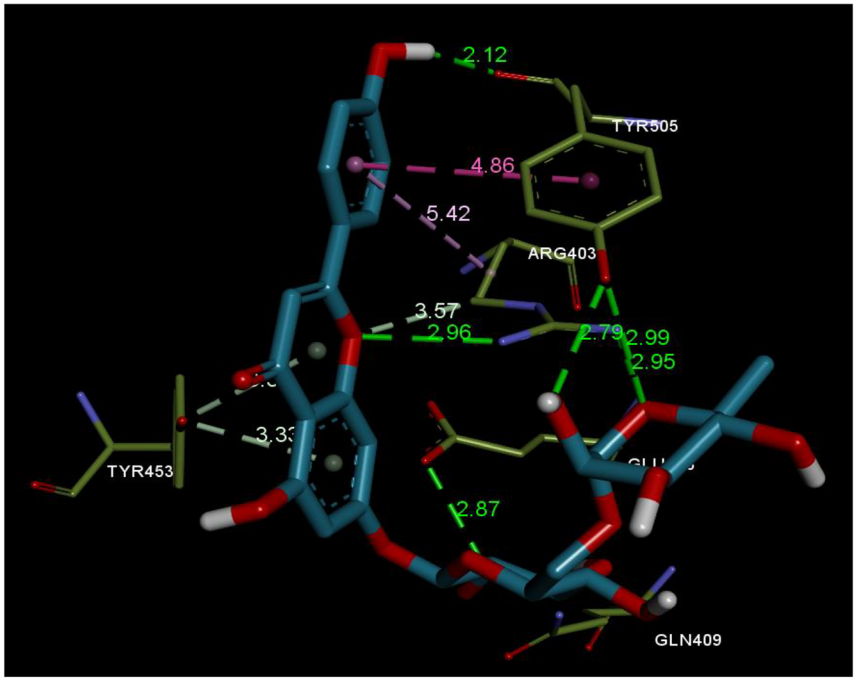

IsorhoifolinΔG -7.9 kcal/mol

Figure 1: Interaction profile of Arq Ajīb phytocompounds and active site residues of SARS-CoV-2 S glycoprotein. Each color of amino acid residues and interaction markers indicates different types of interaction. Green represents a conventional H-bonding, Pink denotes Pi-amide interaction and the rest of them represents weak van der Waals interaction.

Table 3: Amino acid residues of SARS-CoV-2 main protease $3CL^{pro}$ (7BQY) participated in H-Bond and hydrophobic interactions with ligands.

Compound	Binding energy, kcal/mol	Interactions	
		H-bonding	Hydrophobic
Nelfinavir	−7.7	His41, Glu166, Gln189	His41, Cys145, Met165
Thymol	−4.8	His164	His41, Met165
Carvacrol	−4.9	NHB	His41, Met165
Cymene	−4.8	NHB	His41, Met165
Terpinene	−4.8	NHB	Met165
Menthol	−4.6	NHB	His41, Met49, Cys145
Quercetin	−7.9	Glu166, Thr190	His41, Met165, Pro168, Gln189
Isorhoifolin	−8.8	Phe140, Glu166, Thr190	His41, Asn142, Met165, Pro168, Gln189
Camphor	−4.2	Glu166	
Linalool	−4.9	His41	His41, Met49
Borneol	−4.1	His41	Leu27, His41

NHB, no hydrogen bond interactions.

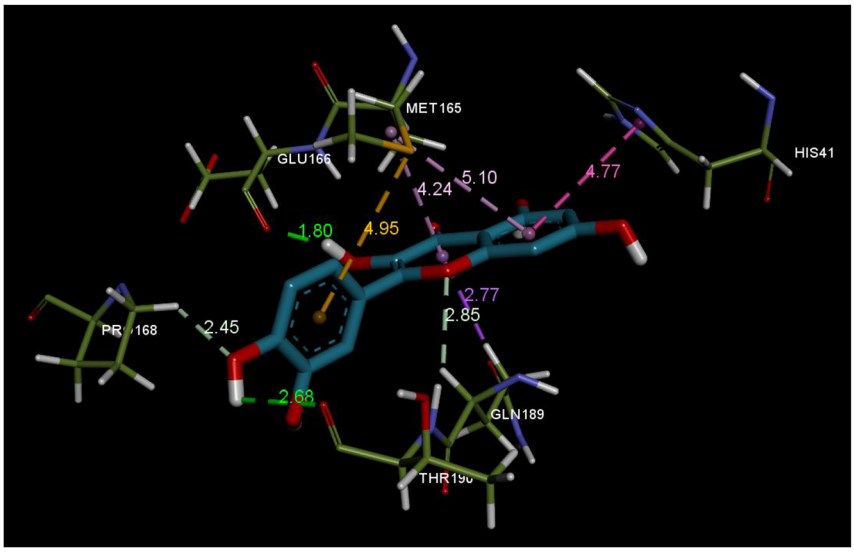

QuercetinΔG -7.9 kcal/mol

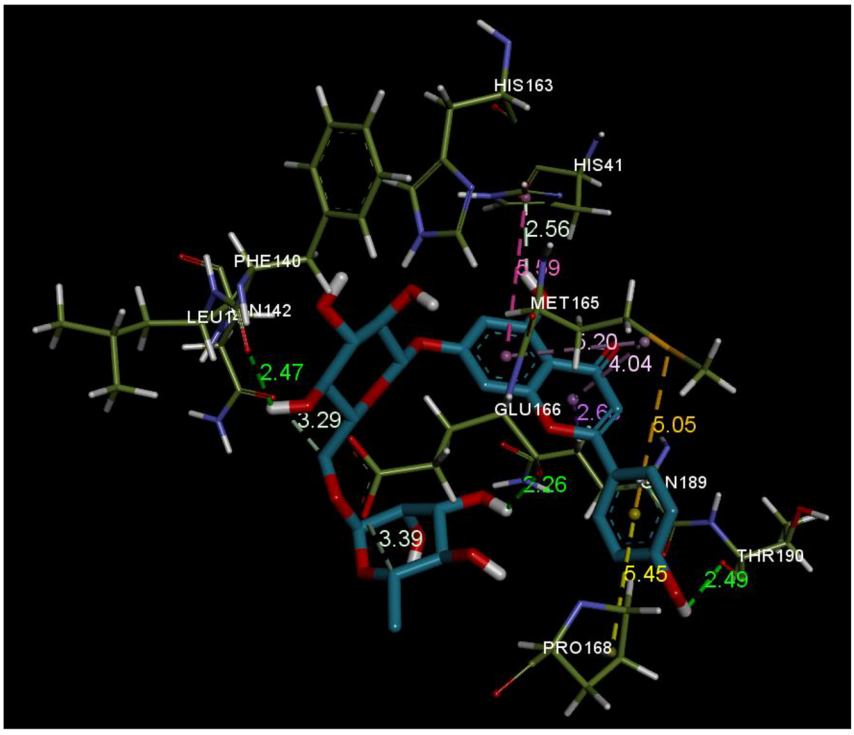

IsorhoifolinΔG -8.8 kcal/mol

Figure 2: Interaction profile of Arq Ajīb phytocompounds and active site residues of SARS-CoV-2 main protease $3CL^{pro}$. Each color of amino acid residues and interaction markers indicates different types of interaction. Green represents a conventional H-bonding, Yellow indicates Pi-SH interaction, Pink denotes Pi-amide interaction and the rest of them represent weak van der Waals interaction.

and Pi–donor with His41, Cys145 and Met165 respectively. Quercetin and Isorhoifolin showed docking energy –7.9 and 8.8 kcal/mol respectively (Table 3). Both the two compounds formed an extensive network of H-bonds within the protease receptor site with Phe140, Glu166 and Thr190 residues and hydrophobic interactions with Gln189, Met165 and Pro168 (Table 3; Figure 2). Visualization performed for phytocompounds having best binding affinity with $3CL^{pro}$ represented in Figure 2. The OH atom of Quercetin, formed H-bond with Glu166 with a bond length of 1.80 Å and Thr190 with bond length 2.68 Å, in addition with hydrophobic interactions of Pi–Sigma, Pi–Sulfur, and Pi–Pi with Glu189, Met165, and His41. Isorhoifolin formed three H-bonding interactions with amino acids Phe140, Glu166 and Thr190 with bond length of 2.47, 2.26 and 2.49 Å respectively, in addition with hydrophobic interactions of Pi–Sigma, Pi–Sulfur, Pi–Pi and Pi–Alkyl with amino acids Glu189, Met165, His41 and Pro168 respectively.

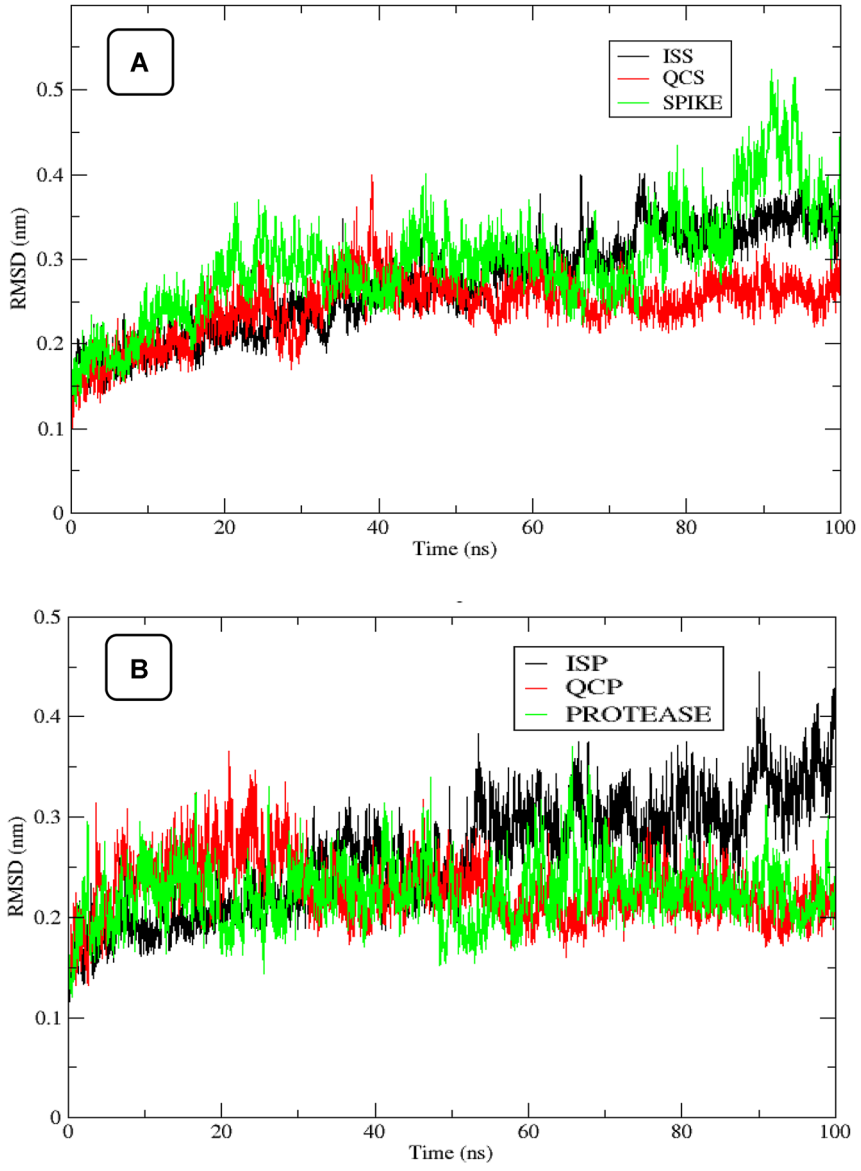

Figure 3: RMSD plot for 100 ns time period to check conformational stability. (A) RMSDs of protein with least – square fit to Spike protein in ISS (Black), QCS (Red) and native spike protein (Green). (B) RMSDs of $3CL^{pro}$ protein with least – square fit to protease in ISP (Black), QCP (Red) and native protein $3CL^{pro}$ (Green).

MD analysis of ligand – protein docked complexes

Molecular dynamics study was carried out for 100 ns for four protein – ligand docked complexes (QCS, ISS, QCP, ISP). The average RMSD value recorded for ISS, QCS and native spike protein was 0.27, 0.24, 0.29 nm respectively (Figure 3A). Both ISS and QCS were stable after 75 ns whereas the native protein showed higher deviation. The average RMSD value recorded for ISP, QCP and native $3CL^{pro}$ was 0.26, 0.23 and 0.22 nm respectively (Figure 3B). QCP was found to be stable after 60 ns whereas ISP showed slightly higher deviation when compared to native $3CL^{pro}$.

RMSF was calculated for C-α atom of protein residues to understand the backbone structure flexibility. The residues, fluctuating during the simulation time for 100 ns were represented by the peaks in RMSF plots (Figure 4). The backbone residues of ISS and QCS showed less fluctuation compared to native spike protein (Figure 4A). The residues, participating in ligand interaction of QCS and ISS were Ala397, Phe400, Ala435, Arg454 and Val401, and Arg509 respectively. The native spike protein showed RMSF value of 0.5 nm with high fluctuation when compared to ISS and QCS. RMSF pattern of both ISP and QCP was found similar to that of native $3CL^{pro}$ (Figure 4B). The residues, involved for stable fluctuations were Ser20, Arg40, Ala206 for ISP and Trp31, Val36, Ser144, Val148 and Met162 for QCP.

The level of compactness or solidity of the structure was determined by Radius of Gyration (*Rg*) and *Rg*-plots. Average *Rg* values of protein backbones for ISS, QCS,

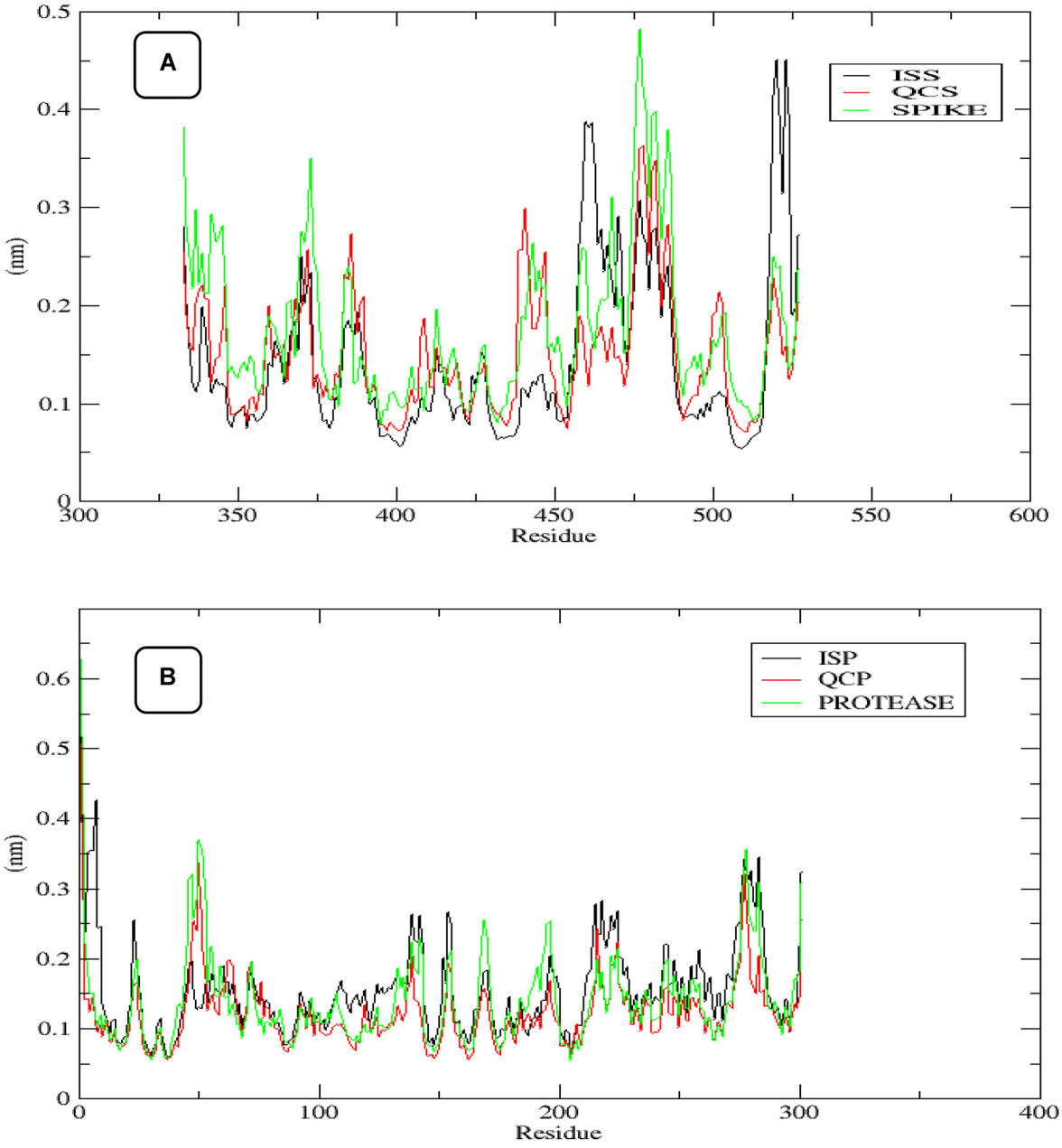

Figure 4: RMSF plot for 100 ns time period to understand the backbone structure flexibility. (A) RMSF of Spike protein in ISS (Black), QCS (Red) and Spike native protein (Green). (B) RMSF of $3CL^{pro}$ protein ISP (Black), QCP (Red) and native $3CL^{pro}$ protein (Green).

native spike, ISP, QCP and native $3CL^{pro}$ were found to be 1.83, 1.83, 1.86, 0.29, 2.21 and 2.19 nm respectively (Figure 5). The results of *Rg* indicate stable simulation between 1.8 and 1.92 nm over the total simulation time (Figure 5A). Ligands bounded to ISS and QCS were able to reach stability earlier than native spike protein. Both ISS and QCS were compact, stable and reach stability after 50 ns. Whereas, *Rg* value for the native $3CL^{pro}$ was fluctuating between 2.13 and 2.27 nm. ISP was found to be stable after 60 ns, whereas, QCP compactness was lower than native $3CL^{pro}$ (Figure 5B).

The specific interactions between ligands and proteins were measured using hydrogen bond formation. The total number of H-bonds formed vs. time is shown in Figure S-1. ISS and QCS exhibited 4 and 5 hydrogen bonds interaction respectively throughout the simulation time (Figure S-1a and b), whereas ISP and QCP exhibited 5 and 4 strong and stable H-bond interaction respectively (Figure S-1c and d).

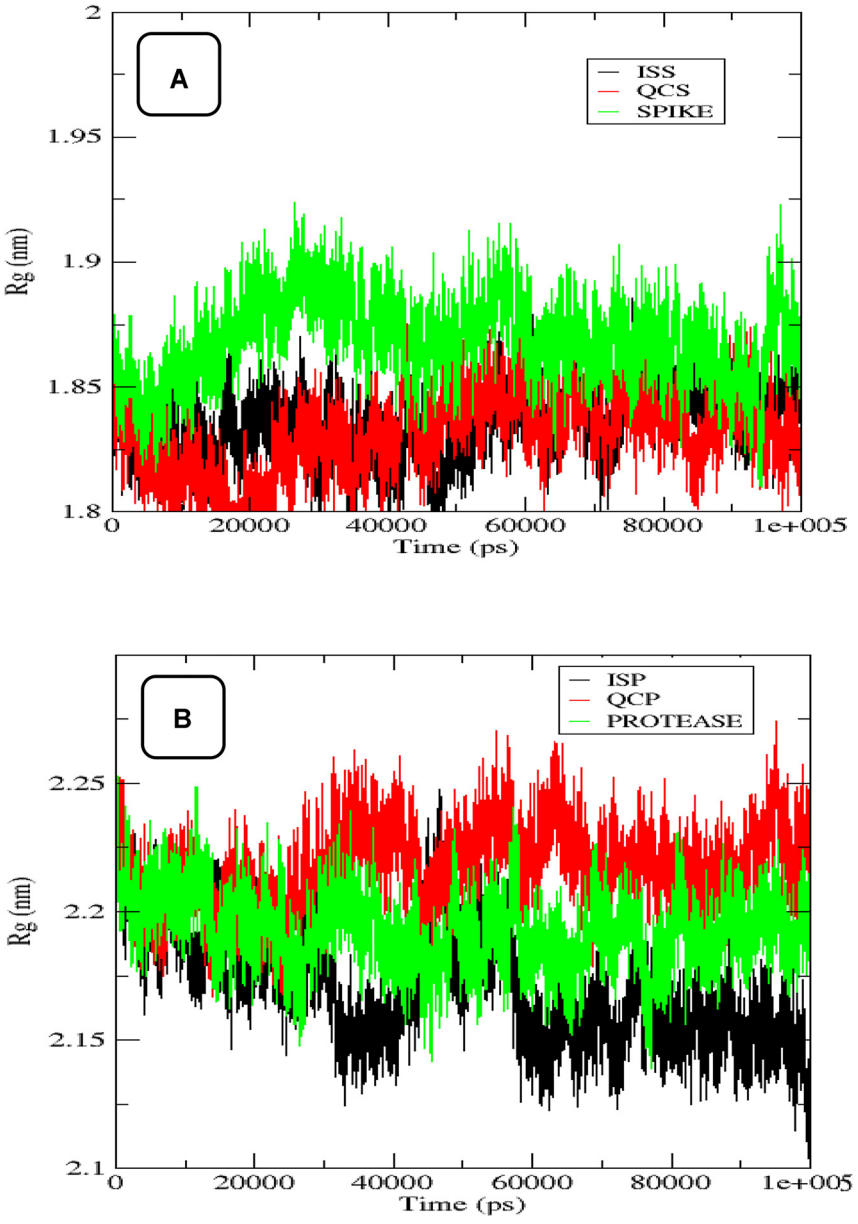

Figure 5: Radius of gyration of the protein backbone atoms. (A) ISS (Black), QCS (Red) and Spike native protein (Green). (B) ISP (Black), QCP (Red) and native $3CL^{pro}$ protein (Green).

The SASA values were found to be similar in case of both ISS and QCS with native protein (Figure S-2a). No significant opening and closing of peaks were found and the ligand remained intact to the protein. QCP exhibited better stability than native $3CL^{pro}$ whereas ISP implied similar peak as that of native $3CL^{pro}$ (Figure S-2b).

The binding free energy for the docked complexes was measured using MM/PBSA calculation method for the last 20 ns (80–100 ns) stable trajectories. Among all the complexes, QCP computed higher binding energy value of –123.153 kJ/mol, whereas ISS, ISP and QCS exhibited binding energy values of –66.583, –28.970 and –24.875 kJ/mol respectively. Along with binding energy, van der Waal energy, electrostatic energy, polar solvation energy, SASA were also calculated for each complex (Table S-2). The energy contribution of protein-ligand complexes was subtracted using MM/PBSA calculation. The bar graph represents residue wise total binding energy contribution for all MD simulated complexes (Figure S-3a–d). It was noted that residues 'Tyr473, Gly476, Cys480, Asn487 and Tyr489' are involved in total energy contribution of QCS Complex (Figure S-3a). The active site residues such as His41, Cys44, Met49, Cys145, Met165 and Thr190 computed for binding energy values of QCP complex (Figure S-3b). It was found that 32 residues were involved in binding energy formation for ISS complex, of which the active site residues were Arg403, Asp405, Arg408, Ile418, Leu455, Phe497, Gln498, Asn501 and Gln506 (Figure S-3c). The binding free energy

for ISP was obtained by 36 residues from which Thr26, Leu27, His41, Asn142, His164, Glu166, Pro168, Arg188, Gln189 and Thr190 were active site residues (Figure S-3d).

Discussion

Computationally, a number of phytocompounds have been reported for significant effects against multiple active targets of SARS-CoV-2 [40, 41]. In the present study, binding affinity and interactions between phytocompounds of Arq Ajīb with potential therapeutic targets of SARS-CoV-2 was evaluated by employing computational tools.

It is established that the SARS-CoV-2 spike protein plays a vital role in facilitating the entry of virus into the host. To recognize and interact with ACE2, SARS-CoV-2 utilizes its S1 CTD, also known as RBD, a key region for interaction with its host receptor. Hence, RBD is considered to be the most important druggable target [7, 8]. The present study predicts that all the tested phytocompounds have good binding affinity with the SARS-CoV-2 spike proteins. Quercetin and Isorhoifolin from *M. arvensis* exhibited significant binding energy, comparable to nelfinavir which was used as positive control. Biological interaction analysis revealed that all docked ligands interacting well with the same amino acid residues as that of hACE2. From the analysis of interactions of the ligand molecules and comparison of energy values it can be predicted that phytocompounds Quercetin and Isorhoifolin interfere well with the binding of spike protein to host cell. Thus, it would not be an embellishment to state that the phytoconstituents present in Arq Ajīb may inhibit the interaction of RBD with the host receptor resulting in the inhibition of virus entry in to the host.

The main protease (M^{pro}/$3CL^{pro}$) is known to play an important role in virus replication as it mediates the proteolytic processing and cleaves the polyprotein to generate various non-structural proteins that are important for viral replication. Therefore, it is considered to be a potential target for the development of targeted drugs against SARS-CoV-2 [42]. The present study predicts that all the tested phytocompounds have good binding affinity with $3CL^{pro}$. Quercetin and Isorhoifolin showed lower binding energy to $3CL^{pro}$, compared to the well-known protease inhibitor, nelfinavir. The result of present study corroborates with the findings of Athira & James, where they reported similar phytocompounds with similar binding energy to $3CL^{pro}$ [43]. Notably, Quercetin and Isorhoifolin have formed extensive network of H-bonds within the active protease receptor site. It indicates that, Quercetin and Isorhoifolin may have the potential to interfere with the proteolytic processing and inhibit the viral replication and transcription.

Molecular dynamics simulation study gives insights in to the binding strength, stability, dynamic equilibration and conformational changes of native proteins with their protein – ligand docked complexes. In the present study, MDS analysis revealed significantly lower RMSD value of QCS and ISS complexes than that of native spike protein, whereas QCP showed similar and ISP showed RMSD value slightly higher to native $3CL^{pro}$. It indicates increased rigidity and stability of QCS, ISS and QCP complexes on binding to their respective native proteins. RMSF pattern, Rg plot and SASA analysis confirmed the stability, solidity and compactness of docked complexes with a higher value in ISS, QCS and QCP complexes. The number of hydrogen bond formation in protein-ligand complexes determines the binding strength and stability of the complex. Based on H-bond formation, QCS and ISP complexes were found to be therapeutically important complexes against respective native proteins. The binding free energy and decomposition analysis revealed significantly higher binding energy of QCP when compared with other three complexes, indicating QCP as potent therapeutic against $3CL^{pro}$.

Quercetin and Isorhoifolin belongs to the subgroup of flavonoid compounds found in a number of medicinal botanicals including *M. arvensis* [44]. In the present study, isorhoifolin exhibited significant binding affinity to both the RBD and main protease, stronger than that of positive control, nelfinavir. However, it is hardly reported for its antiviral activities in previous studies. Quercetin is widely distributed in various plants, vegetables and fruits and is a regular component of a normal diet. It has a great potential in preventing diseases and improving overall health. It has been reported to possess a wide range of biological activities including antiviral, anti-inflammatory, antioxidant and anticancer activities [45]. Wu et al., have reported quercetin as a potent inhibitor of a wide spectrum strains of Influenza A viruses (IAVs) including H1N1, H3N2 and H5N1 viruses, causing seasonal epidemics and pandemics with significant morbidity and mortality. Quercetin inhibited the viral entry in to the host cell via interaction with viral HA protein which is the major glycoprotein of influenza virus responsible for the entry and fusion of virus in to the host. They found that quercetin targeted influenza viral particles instead of the host cell, which indicates that the drug is safe and effective [46]. A recent computational study revealed significant binding affinity of quercetin from *Aloe vera* with RNA-dependent RNA-polymerase with energy value of –9.131 kcal/mol [47]. However, in the present study quercetin exhibited significant binding energy

with S glycoprotein and main protease. It implicate that quercetin may have multitargeted effect on SARS-CoV-2.

Conclusions

The present study was carried out to generate *in silico* evidence for the potential of phytocompounds present in Arq Ajīb against SARS-CoV-2. The present study identifies Quercetin and Isorhoifolin as promising candidates with the potential to interact with Spike glycoprotein and $3CL^{pro}$ and inhibit the viral replication and its entry into the host. However, it has to be substantiated further with *in-vitro* and *in-vivo* studies for the development of safe and effective novel therapeutic agent for COVID-19.

Acknowledgments: Authors acknowledge Director General, CCRUM, Ministry of Ayush, Govt. of India for financial support for this study.
Research funding: Central Council for Research in Unani Medicine, New Delhi, Ministry of Ayush, Govt. of India.
Author contributions: All authors have accepted responsibility for the entire content of this manuscript and approved its submission.
Competing interests: The authors declare no competing interests
Ethical declaration: The present study is a preliminary computational study and does not involve any animal or human subjects; hence it does not involve any ethical and legal dimensions.

References

1. Wang C, Horby PW, Hayden FG, Gao GF. A novel coronavirus outbreak of global health concern. Lancet 2020;395: 470–3.
2. World Health Organization. Coronavirus disease (COVID-19) pandemic; 2021. Available from: https://www.who.int/emergencies/diseases/novel-coronavirus-2019.
3. Reuters. Asia Pacific: India's daily COVID-19 cases pass 400,000 for first time as second wave worsens; 2021. Available from: https://www.reuters.com/world/asia-pacific/india-posts-record-daily-rise-covid-19-cases-401993-2021-05-01/.
4. World Health Organization. World health emergency dashboard: WHO (COVID-19) homepage; 2021. Available from: https://covid19.who.int/region/searo/country/in.
5. Zheng J. SARS-CoV-2: an emerging coronavirus that causes a global threat. Int J Biol Sci 2020;16:1678–85.
6. Nikhat S, Fazil M. Overview of Covid-19; its prevention and management in the light of Unani medicine. Sci Total Environ 2020;728:138859.
7. Wang Q, Zhang Y, Wu L, Niu S, Song C, Zhang Z, et al. Structural and functional basis of SARS-CoV-2 entry by using human ACE2. Cell 2020;181:894–904.
8. Ismail EM, Shantier SW, Mohammed MS, Musa HH, Osman W, Mothana RA. Quinoline and quinazoline alkaloids against COVID-19: an in silico multitarget approach. J Chem 2021;2021: e3613268.
9. Mukherjee PK. Antiviral evaluation of herbal drugs. Qual Control Eval Herbal Drugs 2019;599–628. https://doi.org/10.1016/B978-0-12-813374-3.00016-8.
10. Kiran G, Karthik L, Shree Devi MS, Sathiyarajeswaran P, Kanakavalli K, Kumar KM, et al. In silico computational screening of KabasuraKudineer - official Siddha formulation and JACOM against SARS-CoV-2 spike protein. J Ayurveda Integr Med 2020; 2520:S097530024–94763.
11. CCRUM, Govt. of India. The Unani pharmacopoeia of India, part 2, 1st ed. New Delhi: Central Council for Research in Unani Medicine; 2009, vol 1:5–6 pp.
12. Khan A. Qarabadeen Azam -o- Akmal (Urdu translation). New Delhi: Central Council for Research in Unani Medicine; 2005: 405 p.
13. CCRUM, Govt. of India. Qarabadeen Jadeed. New Delhi: Central Council for Research in Unani Medicine; 2005:152–3 pp.
14. Anwar N, Ahmed NZ, Begum S. Plausible role of Arq Ajib in combating COVID-19: a multifaceted review. J Drug Deliv Therapeut 2021;11:141–8.
15. Khan MA, Khan NA, Qasmi IA, Ahmad G, Zafar S. Protective effect of Arque-Ajeeb on acute experimental diarrhoea in rats. BMC Compl Alternative Med 2004;4:8.
16. Saleem MN, Idris M. Podina (*Mentha arvensis*): transformation from food additive to multifunctional medicine. ARC J Pharmaceut Sci 2016;2:6–15.
17. Thawkar BS, Jawarkar AG, Kalamkar PV, Pawar KP, Kale MK. Phytochemical and pharmacological review of *Mentha arvensis*. Int J Green Pharm 2016;10:71–6.
18. Ghani N. Khazain al-Avia. New Delhi: Idara Kitab al-Shifa; 2011: 478–80, 202–3, 999–1004 pp.
19. Baitar I Kitab al-Jame li Mufradat al-Advia wa al-Aghziya. New Delhi: Central Council for Research in Unani Medicine; 2003, vol 1V:397–9, 379–81, 115–7 pp.
20. Ali AM, Mackeen MM, El-Sharkawy SH, Hamid JA, Ismail NH, Ahmad FB, et al. Antiviral and cytotoxic activities of some plants used in Malaysian indigenous medicine. Pertanika J Trop Agric Sci 1996;19:129–36.
21. Roy S, Chaurvedi P, Chowdhary A. Evaluation of antiviral activity of essential oil of *Trachyspermum Ammi* against Japanese encephalitis virus. Pharmacogn Res 2015;7:263–7.
22. Hussein G, Miyashiro H, Nakamura N, Hattori M, Kakiuchi N, Shimotohno K. Inhibitory effects of sudanese medicinal plant extracts on hepatitis C virus (HCV) protease. Phytother Res 2000; 14:510–6.
23. Bairwa R, Sodha RS, Rajawat BS. *Trachyspermum ammi*. Pharm Rev 2012;6:56–60.
24. Khan MR, Jamal MA, Zeenat F. Therapeutic potential of *Cinnamomum camphora* (Kafoor) in skin disorders: a review. World J Pharmaceut Life Sci 2019;5:108–11.
25. Chen W, Vermaak I, Viljoen A. Camphor–a fumigant during the Black Death and a coveted fragrant wood in ancient Egypt and Babylon–a review. Molecules 2013;18:5434–54.

26. Lee HJ, Hyun EA, Yoon WJ, Kim BH, Rhee MH, Kang HK, et al. In vitro anti-inflammatory and anti-oxidative effects of *Cinnamomum camphora* extracts. J Ethnopharmacol 2006;103:208–16.
27. Tanabe H, Fukutomi R, Yasui K, Kaneko A, Imai S, Nakayama T, et al. Identification of dimethylmatairesinol as an immunoglobulin E-suppressing component of the leaves of *Cinnamomum camphora*. J Health Sci 2011;57:184–7.
28. Pettersen EF, Goddard TD, Huang CC, Couch GS, Greenblatt DM, Meng EC, et al. UCSF Chimera—a visualization system for exploratory research and analysis. J Comput Chem 2004;25:1605–12.
29. Kim S, Thiessen PA, Bolton EE, Chen J, Fu G, Gindulyte A, et al. PubChem substance and compound databases. Nucleic Acids Res 2016;44:D1202–13.
30. ChemAxon. MarvinSketch; 2020. Available from: https://www.chemaxon.com/products/marvin.
31. Trott O, Olson AJ. AutoDock Vina: improving the speed and accuracy of docking with a new scoring function, efficient optimization, and multithreading. J Comput Chem 2010;31:455–61.
32. BIOVIA, Dassault Systèmes, discovery studio visualizer V20.1. San Diego: Dassault Systèmes; 2020. Available from: https://discover.3ds.com/discovery-studio-visualizer-download.
33. Hess B, Kutzner C, van der Spoel D, Lindahl E. GROMACS 4: algorithms for highly efficient, load-balanced, and scalable molecular simulation. J Chem Theor Comput 2008;4:435–47.
34. Schüttelkopf AW, van Aalten DM. PRODRG: a tool for high-throughput crystallography of protein-ligand complexes. Acta Crystallogr D Biol Crystallogr 2004;60:1355–63.
35. Oostenbrink C, Villa A, Mark AE, van Gunsteren WF. A biomolecular force field based on the free enthalpy of hydration and solvation: the GROMOS force-field parameter sets 53A5 and 53A6. J Comput Chem 2004;25:1656–76.
36. Van Der Spoel D, Lindahl E, Hess B, Groenhof G, Mark AE, Berendsen HJ. GROMACS: fast, flexible, and free. J Comput Chem 2005;26:1701–18.
37. Turner PJ. XMGRACE, version 5.1. 19. Beaverton, OR: Center for Coastal and Land-Margin Research, Oregon Graduate Institute of Science and Technology; 2005.
38. Kumari R, Kumar R, Open Source Drug Discovery Consortium, Lynn A. g_mmpbsa–a GROMACS tool for high-throughput MM-PBSA calculations. J Chem Inf Model 2014;54:1951–62.
39. Jin Z, Du X, Xu Y, Deng Y, Liu M, Zhao Y, et al. Structure of M pro from SARS-CoV-2 and discovery of its inhibitors. Nature 2020;582:289–93.
40. Naik B, Gupta N, Ojha R, Singh S, Prajapati VK, Prusty D. High throughput virtual screening reveals SARS-CoV-2 multi-target binding natural compounds to lead instant therapy for COVID-19 treatment. Int J Biol Macromol 2020;160:1–17.
41. Gao LQ, Xu J, Chen SD. In silico screening of potential Chinese herbal medicine against COVID-19 by targeting SARS-CoV-2 3CLpro and angiotensin converting enzyme II using molecular docking. Chin J Integr Med 2020;26:527–32.
42. Tahir Ul Qamar M, Alqahtani SM, Alamri MA, Chen LL. Structural basis of SARS-CoV-2 3CL pro and anti-COVID-19 drug discovery from medicinal plants. J Pharm Anal 2020;10:313–9.
43. Athira Nair D, James TJ. Computational screening of phytocompounds from *Moringa oleifera* leaf as potential inhibitors of SARS-CoV-2 Mpro. Res Square 2020. https://doi.org/10.21203/rs.3.rs-71018/v1.
44. Biswas NN, Saha S, Ali MK. Antioxidant, antimicrobial, cytotoxic and analgesic activities of ethanolic extract of *Mentha arvensis* L. Asian Pac J Trop Biomed 2014;4:792–7.
45. Li Y, Yao J, Han C, Yang J, Chaudhry MT, Wang S, et al. Quercetin, inflammation and immunity. Nutrients 2016;8:167.
46. Wu W, Li R, Li X, He J, Jiang S, Liu S, et al. Quercetin as an antiviral agent inhibits influenza A virus (IAV) entry. Viruses 2015;8:6.
47. Pandit M, Latha N. In silico studies reveal potential antiviral activity of phytochemicals from medicinal plants for the treatment of COVID-19 infection. Res Square 2020. https://doi.org/10.21203/rs.3.rs-22687/v1.

Supplementary Material: The online version of this article offers supplementary material (https://doi.org/10.1515/jcim-2021-0241).